Editors' Suggestion

Atomic Cluster Au_{10}^+ Is a Strong Broadband Midinfrared Chromophore

Alice E. Green,[1] Alexander S. Gentleman,[1] Wieland Schöllkopf,[2] André Fielicke,[2,3,*] and Stuart R. Mackenzie[1,†]
[1]Department of Chemistry, University of Oxford, Physical and Theoretical Chemistry Laboratory, South Parks Road, Oxford OX1 3QZ, United Kingdom
[2]Fritz-Haber-Institut der Max-Planck-Gesellschaft, Faradayweg 4-6, 14195 Berlin, Germany
[3]Institut für Optik und Atomare Physik, Technische Universität Berlin, Hardenbergstr. 36, 10623, Berlin, Germany

(Received 18 December 2020; revised 30 April 2021; accepted 25 May 2021; published 16 July 2021)

We report an intense broadband midinfrared absorption band in the Au_{10}^+ cluster in a region in which only molecular vibrations would normally be expected. Observed in the infrared multiple photon dissociation spectra of $Au_{10}Ar^+$, $Au_{10}(N_2O)^+$, and $Au_{10}(OCS)^+$, the smooth feature stretches 700–3400 cm^{-1} ($\lambda = 14$–2.9 μm). Calculations confirm unusually low-energy allowed electronic excitations consistent with the observed spectra. In $Au_{10}(OCS)^+$, IR absorption throughout the band drives OCS decomposition resulting in CO loss, providing an alternative method of bond activation or breaking.

DOI: 10.1103/PhysRevLett.127.033002

The optical properties of atomically precise metal clusters and nanoparticles continue to attract interest due to their potential in sensing [1], labeling [2], imaging [3], biological [4], and medical applications [5,6]. Gold plays a central role in this activity: the localized surface plasmon resonance in small gold nanoparticles has been well characterized and finds many practical applications [7]. For small gold clusters, a detailed understanding of the electronic and geometric structure offers the prospect of tuning cluster properties, including reactivity.

Here, we report a strong, broad absorption band in the Au_{10}^+ cluster which extends throughout the midinfrared region where only molecular vibrational bands would normally be expected. In the cluster size range studied (Au_n^+, $3 \leq n \leq 12$), this absorption band is unique to $n = 10$ and, remarkably, is preserved when Ar, N_2O, or OCS is adsorbed.

The structures of small charged gas-phase gold clusters have been studied using a wide variety of spectroscopic techniques [8–10]. Using ion mobility mass spectrometry, Kappes and co-workers revealed remarkable planar ground state structures for $n \leq 7$ (Au_n^+) and $n \leq 11$ for Au_n^- clusters [11–13]. Far infrared action spectroscopy of Au_n^+ ($n \leq 9$) recently confirmed these structures [14–16] and visible photodissociation spectroscopy has been used to probe structures around the 2D to 3D transition [17] and other sizes [18–29]. Various studies of ligated clusters also show evidence of this large geometrical change [30–32].

Larger gold clusters exhibit a range of geometrical structures [33,34] from the open Au_{11}^+ structure to close-packed structures, including quasitetrahedral Au_{10}^+ [11] and perfectly tetrahedral Au_{20} [35]. Interestingly, the latter has an anomalously large HOMO-LUMO gap (1.8 eV) [36,37] which, along with the cluster structure, survives cluster deposition onto an ultrathin sodium chloride surface [38]. Petrar *et al.* also predict a large HOMO-LUMO gap (3.88 eV) for Au_{10}^{2+} [39]. The singly occupied molecular orbital (SOMO) to LUMO transition in Au_{10}^+, as a potential carrier for the spectrally broad absorption feature observed, is a key focus of this Letter.

Many structural aspects of gold clusters are explained by electronic shell structures [40,41]. The unpaired 6*s* electron in the gold atom ($[Xe]4f^{14}5d^{10}6s^1$) often leads to it behaving like an alkali metal [42] with delocalization of the valence electrons in clusters leading to magic numbers corresponding to electron (sub)shell closures at $2(1S), 8(1P), 18(1D), 20(2S), \ldots$ within spherical jellium systems [43–46]. Similar shells persist in alternative symmetries [47,48]. In tetrahedral structures, magic numbers arise for $2, 8, 10, 16, 20, \ldots$ electrons with the largest steps in stability at 2, 8, and 20. With 20 valence electrons, Au_{20} comprises a fully stabilized shell favoring a tetrahedral symmetry [35–37,47]. Despite their stability, Au_{20}, and other magic number clusters, can be highly reactive with charge transfer from a support [49,50].

Other gold cluster properties, e.g., the stability of Au_7^+ and Au_9^+ in fragmentation experiments, can also be explained by shell structures [48,51–53]. These properties can be used to tune cluster chemistry. For example, replacing core ligands in a $Au_{11}(PH_3)_7Cl_3$ cluster with O_2 leads to partial electron donation from the 9 valence electron cluster, facilitating CO oxidation [54]. Similar donation explains the fact that only Au_{10}^+ and Au_{22}^+ clusters bind O_2 with a superoxo motif thereby achieving stable 8- and 20-electron structures, respectively [55]. All even n Au_n^+ clusters have unpaired electrons and the literature is rich with odd-even oscillations in physical and chemical properties [34,56–62]. The subject of this study,

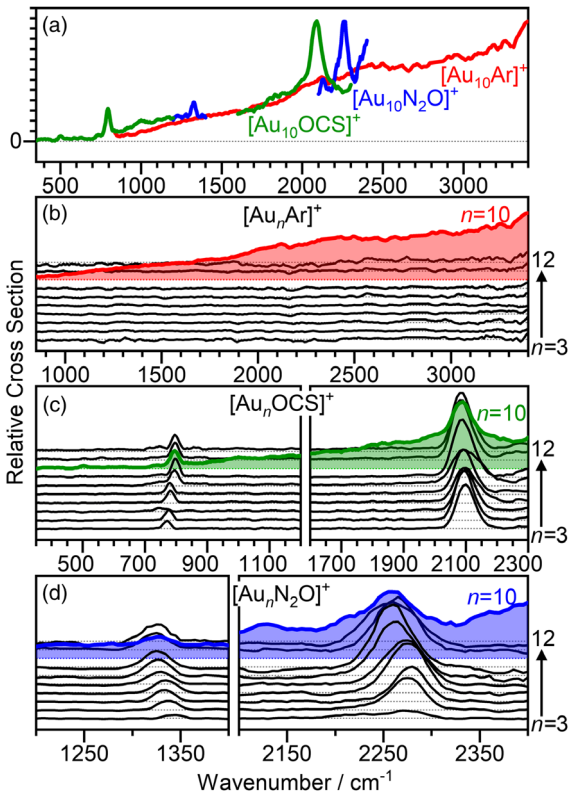

FIG. 1. (a) IRMPD spectra of $[Au_{10}Ar]^+$, $[Au_{10}OCS]^+$, and $[Au_{10}N_2O]^+$ across the midinfrared showing persistent background depletion. (b)–(d) IRMPD spectra of $[Au_nAr]^+$, $[Au_n(OCS)]^+$, and $[Au_n(N_2O)]^+$ ($n = 3$–12), respectively illustrating the unique nature of the $n = 10$ cluster in each case. Intensity is plotted as a relative cross section, corrected for laser power.

Au_{10}^+, with its 9 valence electrons, is shown to exhibit a very small (~0.5 eV) SOMO-LUMO gap with several low-lying optically accessible excited electronic states.

Here, we report a common intense, broad absorption feature in the infrared multiple-photon dissociation (IRMPD) spectra of three isolated $Au_{10}X^+$ systems: $[Au_{10}Ar]^+$, $[Au_{10}OCS]^+$, and $[Au_{10}N_2O]^+$. These show all the characteristics of a low-energy electronic band, and time-dependent density functional theory (TDDFT) simulations confirm an anomalously low SOMO-LUMO gap in Au_{10}^+ with allowed first vertical excitation consistent with the observed band. Full experimental and computational details are given in the Supplemental Material [63], which includes Refs. [64–67] and [68–87], respectively. Briefly, clusters are generated by laser ablation of a gold target and cooled by collision in a clustering channel maintained at 105–300 K. Adsorbates are either introduced via a late mixing valve (OCS, N_2O) [62,88] or seeded in the helium carrier gas (Ar). Previous experiments have shown that clusters thermalize effectively to the temperature of such sources [89].

Figure 1(a) shows the IRMPD spectra in the mid-IR region accessible with the Fritz Haber Institute free-electron laser [64]. The spectra are recorded by loss of the adsorbate and there is no evidence of fragmentation of the metal cluster itself (see Fig. S3 in Supplemental Material [63]). In each system, the spectrum comprises a smooth continuous absorption from 700 cm^{-1} upward and has not reached its peak by 3400 cm^{-1}, the upper limit of our measurements. In $[Au_{10}OCS]^+$ and $[Au_{10}N_2O]^+$, the narrow OCS and N_2O molecular vibrational absorption features are clearly visible on top of this broad background and have been discussed elsewhere [62,88].

Figures 1(b)–1(d) show that this intense, broad absorption band is unique to the $n = 10$ cluster in the $n = 3$–12 range studied here (see also Fig. S3 [63]). For all other cluster sizes, only the vibrational bands of the molecularly adsorbed N_2O or OCS are observed in this range.

The observation of this broad absorption band in the Ar-tagged Au_{10}^+ cluster is revealing. In the absence of molecular chromophores, no vibrational transitions are expected at wave numbers >250 cm^{-1} (see Ref. [14] and Fig. S13, Supplemental Material [63]) suggesting this is a low-energy, Au_{10}^+-centered, electronic absorption. This interpretation is consistent with the same smooth featureless appearance with all three adsorbates. Common in larger clusters and nanoparticles with their higher density of states and bandlike structures, low-energy HOMO-LUMO transitions are unusual in small clusters where shell structures typically lead to larger state separations. Furthermore, these transitions are often either within the same shell or between shells with angular momentum quantum numbers differing by 2, and are thus dipole forbidden.

Low-lying excited electronic states have, however, recently been proposed by Hansen *et al.* [60] to account for short radiative lifetimes of some small Au_n^+ ($n < 20$) clusters, though not particularly $n = 10$. Our IRMPD technique is complementary to this method but sensitive to lower oscillator strengths—the C=O and C=S stretches in $[Au_{10}OCS]^+$, clearly observed in Fig. 1(c) (and Ref. [62]), have oscillator strengths $f = 2 \times 10^{-4}$ and 7×10^{-6}, respectively [90]. This is not the first time that electronic states have been observed by IRMPD, Bakker and co-workers having reported low-energy electronic bands in Ta_5C_3 [91].

It is notable that the systems in which we observe this broad absorption all involve closed-shell adsorbates (Ar, OCS, N_2O). These present minimal perturbation to the electronic structure of the Au_{10}^+. No such feature was observed in the spectra of $[Au_{10}O_2]^+$ or $[Au_{10}NO]^+$ with their open-shell adsorbates [55,92]. With 9 valence electrons, Au_{10}^+ has one more than a stable 8-electron shell [40]. This outer electron is delocalized around the quasitetrahedral structure [11] and readily donates into the π^* orbital of O_2 generating superoxo species [55]. All even n Au_n^+ clusters activate nitric oxide molecules by electron donation into the NO antibonding π^* orbital [92]. Figures S13–S16 of [63] show simulated vibrational and electronic spectra of $[Au_{10}\text{-}L]^+$ (L = Ar, OCS, N_2O, NO, and O_2).

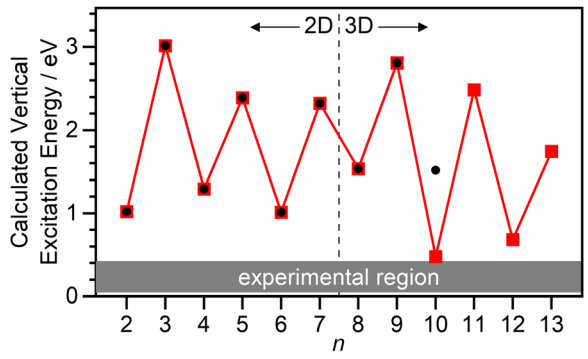

FIG. 2. First vertical excitation energies for Au_n^+ ($n = 2$–13) calculated using TDDFT using the UB3P86–SDD [68–71] functional-basis set combination (including HOMO → LUMO and HOMO-1 → SOMO transitions). Solid black circles indicate excitations from the lowest energy structures, whereas the red squares (and line) are from structures assigned in previous experiments [11,14]. For $n = 2$–9, these are the same structures. For Au_{10}^+, the structure assigned by ion mobility [11] lies 0.05 eV higher than the global minimum (see text and Fig. S5 in Supplemental Material [63] for details). The gray shaded area illustrates the spectral region investigated (Fig. 1).

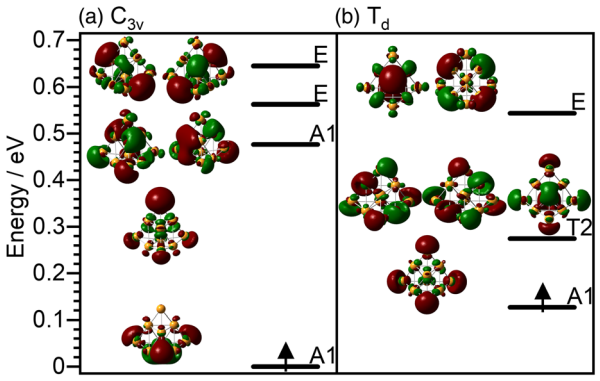

FIG. 3. Orbital visualization of states involved in the lowest vertical transitions from the TDDFT calculations for (a) the Au_{10}^+ structure assigned by ion mobility [11] and (b) a tetrahedrally constrained structure. All are single transitions from the unpaired alpha electron in the SOMO to 5 low-lying states, with degenerate levels indicated. Energies are relative to the ground state of the C_{3v} isomer and the next vertical excitations lie at 2.63 and 2.74 eV for T_d and C_{3v}, respectively.

The structures of gold clusters clearly reflect a complex balance of factors including electronic shell structure, *s-d* hybridization, relativistic effects, and pseudo Jahn-Teller distortion. We have investigated low-energy electronic excitations in low-lying isomers of the clusters studied here by using TDDFT to calculate the first vertical excitation energies. Many clusters in this range exhibit energetically low-lying isomers [11,12,30], and a detailed search was completed for Au_n^+, $n = 2$–10 (see Supplemental Material for structures and vertical excitations of all low-lying isomers found [63]). Figure 2 shows the calculated vertical excitation energies for cluster structures identified by Kappes and co-workers in their ion mobility studies [11], and confirmed in recent far infrared spectroscopic studies ($n \leq 9$) [14]. A pronounced alternation is observed with transitions consistently higher for the (closed-shell) odd n clusters than for adjacent even n clusters.

For Au_{10}^+, density functional theory (DFT) predicts at least five isomers within 0.2 eV of the putative global minimum structure (Fig. S5 [63]). Kappes and co-workers assigned Au_{10}^+ definitively to a distorted tetrahedral isomer whose calculated cross section (77.4 Å^2) matches the ion mobility data (77.8 ± 2 Å^2) better than that of the lowest energy structure (81.8 Å^2) [11]. This quasitetrahedral Au_{10}^+ isomer (which lies 0.05 eV above the putative global minimum) has a particularly low calculated first vertical excitation energy (see Fig. 2) consistent with the spectrum observed here. This is a direct, dipole-allowed SOMO-LUMO transition for which the calculated oscillator strength is high ($f = 0.0019$).

Au_{12}^+ also has a low-energy calculated transition, but we see no evidence in our spectra for an equivalent infrared feature. For some cluster isomers (e.g., $n = 2$, 6, 8) the HOMO-1 → SOMO excitations are lower in energy than the SOMO → LUMO transition, but the oscillator strengths for such transitions are typically markedly lower (see Figs. S8, S9, and S12 [63]).

The presence of allowed low-lying electronic transitions in 9 valence electron Au_{10}^+ can be better understood in terms of a combination of electronic and geometrical structure as illustrated in Fig. 3, which shows the calculated low-lying states involved, arising primarily from the 10 Au 6*s* orbitals. The experimentally determined structure is a pseudo Jahn-Teller distorted tetrahedron [11]. The SOMO orbital in Au_{10}^+ is highly diffuse and the HOMO-1 → SOMO gap large (>3 eV from ground state orbital energies) reflecting the stability of the 8-electron system. In T_d, unlike in spherical symmetry, the $2S$ symmetry adapted orbital lies just below $1D$, which is split into $E \oplus T_2$ components [47] (and then further to $A_1 \oplus E \oplus E$ in distortion to C_{3v}), leading to the anomalously low SOMO-LUMO gap for such a small cluster. The strong state mixing driven by the distortion, coupled with the lack of inversion symmetry, provides the oscillator strength to a transition which, in spherical symmetry, would be dipole forbidden. Tables S3 and S4 (Supplemental Material [63]) give calculated oscillator strengths for the lowest energy (<0.7 eV) transitions involved which increase by a factor 3.7 upon $T_d \rightarrow C_{3v}$ distortion as all transitions $A_1 \rightarrow A_1, E, E$ become allowed.

Figure 4(a) shows a summary of the calculated lowest energy electronic transitions of Au_n^+ ($n = 2$–13) and their corresponding oscillator strengths, including the predicted low-energy transitions of Au_{10}^+ shown in Fig. 3. Figures 4(b) and 4(c) represent an attempt to (i) fit the full spectrum of the electronic band and (ii) use it to compare

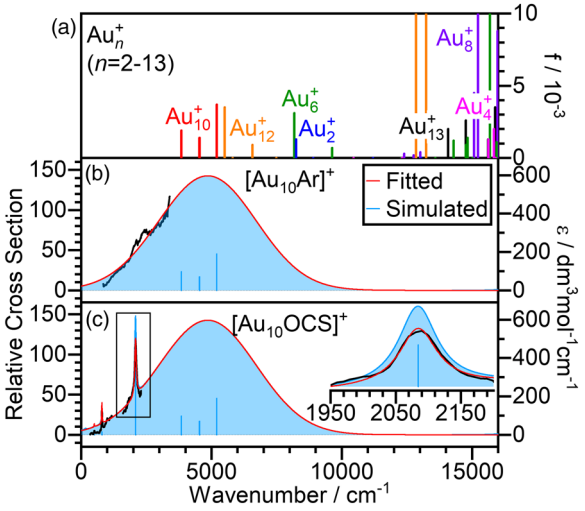

FIG. 4. (a) Calculated low-energy vertical excitations of Au_n^+ ($n = 2$–13) assuming structures assigned in previous experiments [11,14]. (b),(c) IRMPD spectra of $[Au_{10}Ar]^+$ and $[Au_{10}OCS]^+$, respectively (black lines), and corresponding fits in red. Calculated bands are reported as ε, the molar absorption coefficient, and blue shaded areas give the overall simulated spectra with individual peak centers marked. Inset: Relative intensity of the OCS vibrational band at 2084 cm^{-1} (C=O stretch) assuming fitting of the electronic band. Further fitting details are given in the Supplemental Material [63].

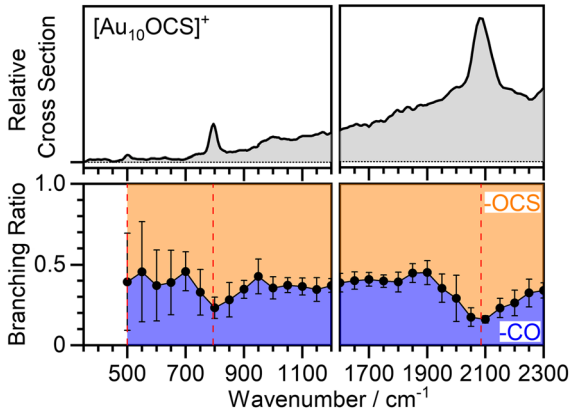

FIG. 5. Branching ratio for CO loss following photodissociation of $[Au_{10}OCS]^+$ recorded in enhancement of $[Au_{10}S]^+$. Uncertainties reflect the standard deviation of the averaging applied. Dashed lines indicate $[Au_{10}OCS]^+$ molecular vibrational bands.

the calculated oscillator strengths for the electronic and vibrational bands in $[Au_{10}OCS]^+$ with those observed experimentally.

Clearly, we have not recorded the entire Au_{10}^+ absorption band here. Nevertheless, following Gloess *et al.* [17] and Shayeghi *et al.* [93], Figs. 4(b) and 4(c) show that Gaussian profiles centered on the calculated vertical excitation energies of Au_{10}^+ account well for the spectrum observed and permit an estimate of the width of the spectral band of 4410 cm^{-1} (ca. 0.55 eV). Several factors likely contribute to this spectral width. The state mixing arising from the pseudo Jahn-Teller deformation leads to avoided crossings between the states involved. In addition to providing a strong transition strength dependence on this deformation coordinate, this provides a mechanism for rapid, diabatic crossing back to the ground state leading to lifetime broadening.

The relative intensities of the simulated vibrational and electronic components of the spectra are compared in Fig. 4(c). By way of example, we have used the $Au_{10}Ar^+$ fit for the electronic band to extract linewidths of 71, 24, and 20 cm^{-1} for the OCS fundamental modes in $[Au_{10}OCS]^+$ at ca. 500, 795, and 2084 cm^{-1}, respectively. Using these linewidths, the calculated relative oscillator strengths of the electronic (Au_{10}^+-centered) and vibrational ($[Au_{10}OCS]^+$) contributions show excellent agreement with the experimental spectrum [see Fig. 4(c), inset] providing some confidence in the simulations.

In addition to capturing the observed Au_{10}^+ band, our TDDFT simulations predict a similar set of low-lying electronically excited states for Au_{12}^+ [see Fig. 4(a)]. In this case an allowed SOMO-LUMO band is predicted ca. 0.2 eV higher than that in Au_{10}^+. We find no evidence in our spectra for such a band, but this may simply indicate a narrower spectral linewidth which is likely to be different for each cluster size and/or transition. It would be interesting to search further to the blue for such a band. For comparison, electronic bands in the visible (2–3 eV) region for Au_7^+, Au_8^+, and Au_9^+ have typical spectral widths of 0.11–0.16 eV [17].

We have previously reported infrared-induced bond breaking in $[Au_nOCS]^+$ (even n) entrance channel complexes following pumping of the OCS vibrational modes [62]. In $[Au_{10}OCS]^+$, both simple OCS loss and CO loss (reflecting OCS decomposition) are observed throughout the broad absorption band reported here. Figure 5 shows the branching ratio for the CO loss (i.e., reactive channel) as the absolute enhancement in the $Au_{10}S^+$ signal as a fraction of $[Au_{10}OCS]^+$ depletion. Clearly, electronic excitation (e.g., in the region 900–1900 cm^{-1}) drives bond-breaking chemistry every bit as efficiently as does direct vibrational pumping (at 795 ± 20 and 2084 ± 50 cm^{-1}).

It is likely that both vibrational and electronic absorption ultimately result in the simple heating of the parent cluster until either the $[Au_{10}$--$SCO]^+$ or $[Au_nS$--$CO]^+$ dissociation limit is reached. For even n clusters, the OCS binding energy (ca. 0.5 eV) is comparable with the highest barrier along the OCS dissociation coordinate [62]. We have not undertaken an intensity-dependence study, but, under the conditions employed here, the average cluster has significant internal energy and even one or two photons in this spectral region (0.1–0.3 eV) is likely to be sufficient to drive fragmentation on the microsecond timescale required. It is equally possible, however, that the excited electronic state, although having the same multiplicity as the ground state, could lead to interesting new chemistry. As indicated by the orbital

visualization in Fig. 3, the electronic excitation drives charge transfer from gold atoms within the cluster to the apex atoms at which OCS preferentially binds. Certainly, the branching ratio for CO loss is higher (ca. 0.4) in regions of electronic excitation than in spectral regions in which OCS vibrations are excited (around 2084 and 795 cm^{-1}).

This is the first time we have observed bond-breaking chemistry on the surface of a cluster driven by infrared electronic excitation. Freed from the need to excite discrete vibrational quanta, this could lead to interesting cluster surface chemistry such as identification of reactive thresholds and simultaneous excitation of different adsorbates. Unique to $n = 10$ in the Au_n^+ size range studied ($n \leq 12$) this low-lying electronic absorption band makes this an attractive system with which to explore the gas-phase reactivity on different potential energy surfaces.

Any ability to harness these unusual photochemical properties of Au_{10}^+ for any practical application is, however, likely to depend on the extent to which they survive ligand stabilization in solution [94,95] or deposition onto a suitable substrate [96]. In this context, by soft-landing clusters in neon matrices, Brune and co-workers have shown that the intense fluorescence of ligand-protected (or protein encapsulated) Au_{20} clusters is intrinsic to the naked Au_{20} moiety [97]. Significant recent progress has also been made in our understanding of charge control in model catalytic systems [98–100], and extensive work has characterized the reactivity of size-selected gold clusters deposited from the gas phase [49,50,101]. Notably, Au_8 clusters on MgO(001) become negatively charged and promote CO oxidation. Au_8^- is, of course, isoelectronic with Au_{10}^+. In terms of geometrical structure, scanning tunneling microscopy has shown that the low-energy pyramidal form of Au_{20} survives deposition from the gas phase onto a NaCl film [38].

It is clear that further experiments remain to fully characterize this unusual spectral feature in Au_{10}^+, not least to determine the full spectrum. However, it is hoped that even the observations reported here—in particular, the potential for photocatalytic chemistry illustrated in Fig. 5—provide sufficient incentive to encourage the surface cluster and nanoparticle community to explore this intriguing system in more detail.

This work was funded by EPSRC under Programme Grants No. EP/L005913 and No. EP/T021675. A. E. G. is supported by a Leon and Iris Beghian Scholarship through Magdalen College, Oxford. A. F. thanks the Deutsche Forschungsgemeinschaft for a Heisenberg Grant (No. FI 893/5) and the Max-Planck-Gesellschaft. We are grateful to John McGrady and Aras Kartouzian for useful discussions.

*Corresponding author.
fielicke@fhi-berlin.mpg.de
†Corresponding author.
stuart.mackenzie@chem.ox.ac.uk

[1] L. Zhang and E. Wang, Nano Today **9**, 132 (2014).
[2] C. A. J. Lin *et al.*, ACS Nano **3**, 395 (2009).
[3] H. Liu *et al.*, Adv Mater **31**, 1901015 (2019).
[4] S. Choi, R. M. Dickson, and J. Yu, Chem. Soc. Rev. **41**, 1867 (2012).
[5] C. Zhou, M. Long, Y. Qin, X. Sun, and J. Zheng, Angew. Chem. Int. Ed. **50**, 3168 (2011).
[6] J. B. Vines, J. H. Yoon, N. E. Ryu, D. J. Lim, and H. Park, Front. Chem. **7**, 167 (2019).
[7] V. Amendola, R. Pilot, M. Frasconi, O. M. Maragò, and M. A. Iatì, J. Phys. Condens. Matter **29**, 203002 (2017).
[8] M. P. Johansson, A. Lechtken, D. Schooss, M. M. Kappes, and F. Furche, Phys. Rev. A **77**, 053202 (2008).
[9] X. Xing, B. Yoon, U. Landman, and J. H. Parks, Phys. Rev. B **74**, 165423 (2006).
[10] H. Häkkinen, B. Yoon, U. Landman, X. Li, H.-J. Zhai, and L.-S. Wang, J. Phys. Chem. A **107**, 6168 (2003).
[11] S. Gilb, P. Weis, F. Furche, R. Ahlrichs, and M. M. Kappes, J. Chem. Phys. **116**, 4094 (2002).
[12] P. Weis, T. Bierweiler, E. Vollmer, and M. M. Kappes, J. Chem. Phys. **117**, 9293 (2002).
[13] F. Furche, R. Ahlrichs, P. Weis, C. Jacob, S. Gilb, T. Bierweiler, and M. M. Kappes, J. Chem. Phys. **117**, 6982 (2002).
[14] P. Ferrari, G. L. Hou, O. V. Lushchikova, F. Calvo, J. M. Bakker, and E. Janssens, Phys. Chem. Chem. Phys. **22**, 11572 (2020).
[15] A. Shayeghi, R. Schäfer, D. M. Rayner, R. L. Johnston, and A. Fielicke, J. Chem. Phys. **143**, 024310 (2015).
[16] A. Shayeghi, R. L. Johnston, D. M. Rayner, R. Schafer, and A. Fielicke, Angew. Chem. Int. Ed. **54**, 10675 (2015).
[17] A. N. Gloess, H. Schneider, J. M. Weber, and M. M. Kappes, J. Chem. Phys. **128**, 114312 (2008).
[18] M. Förstel, K. M. Pollow, K. Saroukh, E. A. Najib, R. Mitric, and O. Dopfer, Angew. Chem. Int. Ed. **59**, 21403 (2020).
[19] M. Förstel, B. K. A. Jaeger, W. Schewe, P. H. A. Sporkhorst, and O. Dopfer, Rev. Sci. Instrum. **88**, 123110 (2017).
[20] M. Förstel, W. Schewe, and O. Dopfer, Angew. Chem. Int. Ed. **58**, 3356 (2019).
[21] V. E. Kaydashev, E. Janssens, and P. Lievens, J. Chem. Phys. **142**, 034310 (2015).
[22] V. Kaydashev, P. Ferrari, C. Heard, E. Janssens, R. L. Johnston, and P. Lievens, Part. Part. Syst. Charact. **33**, 364 (2016).
[23] S. M. Lang, P. Claes, N. T. Cuong, M. T. Nguyen, P. Lievens, and E. Janssens, J. Chem. Phys. **135**, 224305 (2011).
[24] A. Shayeghi, L. F. Pašteka, D. A. Götz, P. Schwerdtfeger, and R. Schäfer, Phys. Chem. Chem. Phys. **20**, 9108 (2018).
[25] A. Shayeghi, C. J. Heard, R. L. Johnston, and R. Schäfer, J. Chem. Phys. **140**, 054312 (2014).
[26] A. Shayeghi, R. L. Johnston, and R. Schäfer, Phys. Chem. Chem. Phys. **15**, 19715 (2013).
[27] A. Schweizer, J. M. Weber, S. Gilb, H. Schneider, D. Schooss, and M. M. Kappes, J. Chem. Phys. **119**, 3699 (2003).
[28] B. K. A. Jaeger, M. Savoca, O. Dopfer, and N. X. Truong, Int. J. Mass Spectrom. **402**, 49 (2016).

[29] B. A. Collings, K. Athanassenas, D. Lacombe, D. M. Rayner, and P. A. Hackett, J. Chem. Phys. **101**, 3506 (1994).
[30] A. Fielicke, G. von Helden, G. Meijer, D. B. Pedersen, B. Simard, and D. M. Rayner, J. Am. Chem. Soc. **127**, 8416 (2005).
[31] G. Dietrich, S. Krückeberg, K. Lützenkirchen, L. Schweikhard, and C. Walther, J. Chem. Phys. **112**, 752 (2000).
[32] K. Sugawara, F. Sobott, and A. B. Vakhtin, J. Chem. Phys. **118**, 7808 (2003).
[33] A. P. Woodham and A. Fielicke, in *Gold Clusters, Colloids and Nanoparticles I. Structure and Bonding*, edited by D. Mingos (Springer, Berlin, 2013), https://doi.org/10.1007/430_2013_136.
[34] H. Häkkinen, Chem. Soc. Rev. **37**, 1847 (2008).
[35] P. Gruene, D. M. Rayner, B. Redlich, A. F. G. van der Meer, J. T. Lyon, G. Meijer, and A. Fielicke, Science **321**, 674 (2008).
[36] J. Li, X. Li, H. J. Zhai, and L. S. Wang, Science **299**, 864 (2003).
[37] J. Wang, G. Wang, and J. Zhao, Chem. Phys. Lett. **380**, 716 (2003).
[38] Z. Li *et al.*, Sci. Adv. **6**, eaay4289 (2020).
[39] P. M. Petrar, M. B. Sárosi, and R. B. King, J. Phys. Chem. Lett. **3**, 3335 (2012).
[40] H. Häkkinen, Adv. Phys. X **1**, 467 (2016).
[41] M. G. Mayer, Science **145**, 999 (1964).
[42] W. D. Knight, K. Clemenger, W. A. de Heer, W. A. Saunders, M. Y. Chou, and M. L. Cohen, Phys. Rev. Lett. **52**, 2141 (1984).
[43] M. Koskinen, P. O. Lipas, and M. Manninen, Z. Phys. D **35**, 285 (1995).
[44] W. Ekardt, Phys. Rev. B **29**, 1558 (1984).
[45] W. A. de Heer, Rev. Mod. Phys. **65**, 611 (1993).
[46] D. E. Bergeron, A. W. Castleman, Jr., T. Morisato, and S. N. Khanna, Science **304**, 84 (2004).
[47] T. Tsukamoto, N. Haruta, T. Kambe, A. Kuzume, and K. Yamamoto, Nat. Commun. **10**, 3727 (2019).
[48] E. Janssens, H. Tanaka, S. Neukermans, R. E. Silverans, and P. Lievens, New J. Phys. **5**, 46 (2003).
[49] M. Arenz, U. Landman, and U. Heiz, ChemPhysChem **7**, 1871 (2006).
[50] B. Yoon, H. Häkkinen, U. Landman, A. S. Wörz, J. M. Antonietti, S. Abbet, K. Judai, and U. Heiz, Science **307**, 403 (2005).
[51] N. Veldeman, E. Janssens, K. Hansen, J. De Haeck, R. E. Silverans, and P. Lievens, Faraday Discuss. **138**, 147 (2008).
[52] P. Ferrari, H. A. Hussein, C. J. Heard, J. Vanbuel, R. L. Johnston, P. Lievens, and E. Janssens, Phys. Rev. A **97**, 052508 (2018).
[53] K. Hansen, A. Herlert, L. Schweikhard, and M. Vogel, Phys. Rev. A **73**, 063202 (2006).
[54] O. Lopez-Acevedo, K. A. Kacprzak, J. Akola, and H. Häkkinen, Nat. Chem. **2**, 329 (2010).
[55] A. P. Woodham and A. Fielicke, Angew. Chem. Int. Ed. **53**, 6554 (2014).
[56] J. K. Gibson, J. Vac. Sci. Technol. A **16**, 653 (1998).
[57] A. Herlert, S. Krückeberg, L. Schweikhard, M. Vogel, and C. Walther, J. Electron Spectrosc. Relat. Phenom. **106**, 179 (2000).
[58] S. Becker *et al.*, Z. Phys. D **30**, 341 (1994).
[59] I. Katakuse, T. Ichihara, Y. Fujita, T. Matsuo, T. Sakurai, and H. Matsuda, Int. J. Mass Spectrom. Ion Process. **67**, 229 (1985).
[60] K. Hansen, P. Ferrari, E. Janssens, and P. Lievens, Phys. Rev. A **96**, 022511 (2017).
[61] E. M. Fernández, J. M. Soler, I. L. Garzón, and L. C. Balbás, Phys. Rev. B **70**, 165403 (2004).
[62] A. E. Green, S. Schaller, G. Meizyte, B. J. Rhodes, S. P. Kealy, A. S. Gentleman, W. Schöllkopf, A. Fielicke, and S. R. Mackenzie, J. Phys. Chem. A **124**, 5389 (2020).
[63] See Supplemental Material at http://link.aps.org/supplemental/10.1103/PhysRevLett.127.033002 for further experimental details, additional IRMPD data, and comprehensive computational results.
[64] W. Schöllkopf, S. Gewinner, H. Junkes, A. Paarmann, G. von Helden, H. Bluem, and A. M. M. Todd, Proc. SPIE Int. Soc. Opt. Eng. **9512**, 95121L (2015).
[65] A. Yanagimachi, K. Koyasu, D. Y. Valdivielso, S. Gewinner, W. Schöllkopf, A. Fielicke, and T. Tsukuda, J. Phys. Chem. C **120**, 14209 (2016).
[66] N. X. Truong, M. Haertelt, B. K. A. Jaeger, S. Gewinner, W. Schöllkopf, A. Fielicke, and O. Dopfer, Int. J. Mass Spectrom. **395**, 1 (2016).
[67] A. E. Green, J. Justen, W. Schöllkopf, A. S. Gentleman, A. Fielicke, and S. R. Mackenzie, Angew. Chem. Int. Ed. **57**, 14822 (2018).
[68] A. D. Becke, J. Chem. Phys. **98**, 5648 (1993).
[69] J. P. Perdew, Phys. Rev. B **33**, 8822 (1986).
[70] T. H. Dunning and P. J. Hay, in *Modern Theoretical Chemistry*, edited by H. F. Schaefer (Springer, Boston, MA, 1977), https://doi.org/10.1007/978-1-4757-0887-5_1.
[71] D. Andrae, U. Häußermann, M. Dolg, H. Stoll, and H. Preuß, Theor. Chim. Acta **77**, 123 (1990).
[72] M. J. Frisch *et al.*, *Gaussian 09, Revision D.01* (Gaussian, Inc., Wallingford, 2013).
[73] M. A. Addicoat and G. F. Metha, J. Comput. Chem. **30**, 57 (2009).
[74] F. Weigend and R. Ahlrichs, Phys. Chem. Chem. Phys. **7**, 3297 (2005).
[75] C. Lee, W. Yang, and R. G. Parr, Phys. Rev. B **37**, 785 (1988).
[76] B. Miehlich, A. Savin, H. Stoll, and H. Preuss, Chem. Phys. Lett. **157**, 200 (1989).
[77] T. Yanai, D. P. Tew, and N. C. Handy, Chem. Phys. Lett. **393**, 51 (2004).
[78] J. P. Perdew, J. Tao, V. N. Staroverov, and G. E. Scuseria, J. Chem. Phys. **120**, 6898 (2004).
[79] J. Tao, J. P. Perdew, V. N. Staroverov, and G. E. Scuseria, Phys. Rev. Lett. **91**, 146401 (2003).
[80] J. P. Perdew, K. Burke, and M. Ernzerhof, Phys. Rev. Lett. **77**, 3865 (1996).
[81] J. P. Perdew, K. Burke, and M. Ernzerhof, Phys. Rev. Lett. **78**, 1396(E) (1997).
[82] Y. Zhao and D. G. Truhlar, J. Chem. Phys. **125**, 194101 (2006).
[83] S. Grimme, J. Antony, S. Ehrlich, and H. Krieg, J. Chem. Phys. **132**, 154104 (2010).
[84] S. Grimme, S. Ehrlich, and L. Goerigk, J. Comput. Chem. **32**, 1456 (2011).

[85] G. Herzberg, *Spectra of Diatomic Molecules, Molecular Spectra and Molecular Structure* Vol. I (Krieger Publishing Company, Malabar, FL, 1989).
[86] G. Herzberg, Infrared and Raman Spectra of Polyatomic Molecules, *Molecular Spectra and Molecular Structure* Vol. II (Krieger Publishing Company, Malabar, FL, 1991).
[87] T. Shimanouchi, *Tables of Molecular Vibrational Frequencies Consolidated,* National Standard Reference Data Series Vol. 1 (National Bureau of Standards, Washington, DC, 1972).
[88] E. M. Cunningham *et al.*, Phys. Chem. Chem. Phys. **23**, 329 (2021).
[89] B. A. Collings, A. H. Amrein, D. M. Rayner, and P. A. Hackett, J. Chem. Phys. **99**, 4174 (1993).
[90] A. Komornicki and R. L. Jaffe, J. Chem. Phys. **71**, 2150 (1979).
[91] V. Chernyy, R. Logemann, A. Kirilyuk, and J. M. Bakker, ChemPhysChem **19**, 1424 (2018).
[92] A. Fielicke, G. von Helden, G. Meijer, B. Simard, and D. M. Rayner, Phys. Chem. Chem. Phys. **7**, 3906 (2005).
[93] A. Shayeghi, R. L. Johnston, and R. Schäfer, J. Chem. Phys. **141**, 181104 (2014).
[94] G. Schmid, Chem. Soc. Rev. **37**, 1909 (2008).
[95] H.-F. Zhang, M. Stender, R. Zhang, C. Wang, J. Li, and L.-S. Wang, J. Phys. Chem. B **108**, 12259 (2004).
[96] S. Vajda and M. G. White, ACS Catal. **5**, 7152 (2015).
[97] C. Yu, W. Harbich, L. Sementa, L. Ghiringhelli, E. Apra, M. Stener, A. Fortunelli, and H. Brune, J. Chem. Phys. **147**, 074301 (2017).
[98] A. S. Wörz, U. Heiz, F. Cinquini, and G. Pacchioni, J. Phys. Chem. B **109**, 18418 (2005).
[99] W. D. Schneider, M. Heyde, and H. J. Freund, Chem. Eur. J. **24**, 2317 (2018).
[100] G. Pacchioni and H. J. Freund, Chem. Soc. Rev. **47**, 8474 (2018).
[101] A. Sanchez, S. Abbet, U. Heiz, W. D. Schneider, H. Häkkinen, R. N. Barnett, and U. Landman, J. Phys. Chem. A **103**, 9573 (1999).